Experimental Assessment of Damping in Low Aspect Ratio, Reinforced Concrete Shear Wall Structure

Prepared by C.R. Farrar, J.G. Bennet

Los Alamos National Laboratory

Experimental Assessment of Damping in Low Aspect Ratio, Reinforced Concrete Shear Wall Structure

Prepared by
C.R. Farrar, J.G. Bennet

Los Alamos National Laboratory
Los Alamos, NM 87545

TABLE OF CONTENTS

LIST OF TABLES

LIST OF FIGURES

EXPERIMENTAL ASSESSMENT OF DAMPING IN LOW ASPECT RATIO,
REINFORCED CONCRETE SHEAR WALL STRUCTURES

by

Charles R. Farrar and Joel G. Bennett

ABSTRACT

This report summarizes the experimental data obtained
from the Seismic Category 1 Structures Program concerning
damping in low aspect ratio, reinforced concrete shear wall
structures. This program, that is sponsored by the United
States Nuclear Regulating Research, has tested 37 shear wall
structures and structures and structural elements both
statically (monotonic and cyclic) and dynamically (sine
sweep, random, simulated seismic, and impulse). Data from
these tests have been analyzed by four different methods to
determine equivalent viscous damping ration that can be used
in the analysis of shear wall structures. These methods
are: (1) Frequency response function analysis, (2) The log
decrement method, (3) The hysteretic energy loss method,
and (4) The flow response spectra matching method. The
floor response spectra matching method is, to the author's
knowledge, new and provides the most general method for
assessing a variety of damping mechanisms. Results from the
various methods were generally consistent and the damping
values were found to be in the range specified by current
regulatory guides. A discussion of the various damping
mechanisms, how damping mechanisms effect the equations of
motion, the effects of the type of loading on the various
methods used to determine the damping, and other investiga-
tors results are also presented.

I. INTRODUCTION

The Seismic Category I Structures Program is being carried out at the Los
Alamos National Laboratory under sponsorship of the USNRC, Office of Nuclear
Regulatory Research. The program has the objective of investigating the

1

structural dynamic response of Seismic Category I reinforced concrete structures (exclusive of containment) that are subjected to seismic excitations beyond their design basis. Included in the program objectives is a task to quantify the changes in damping that occur when a structure's response goes from the elastic to the inelastic range. To obtain the necessary information to meet this objective as well as other program objectives, 37 structures and structural elements have been tested statically (monotonic and cyclic) and dynamically (sine sweep, random, simulated seismic, and impulse). This report will summarize the experimental data obtained from these tests concerning damping in reinforced concrete shear wall structures.

The first test specimens to be investigated were one- and two-story, microconcrete, shear wall elements (Fig. 1). These structural elements were tested statically (both monotonic and cyclic) and dynamically with sine sweep, random, and simulated seismic base inputs. For all the structures tested in this program, the simulated seismic inputs were time-scaled versions of the

(a) ONE-STORY SHEAR WALL   (b) TWO-STORY SHEAR WALL

NOTE: 1 in. = 25.4 mm
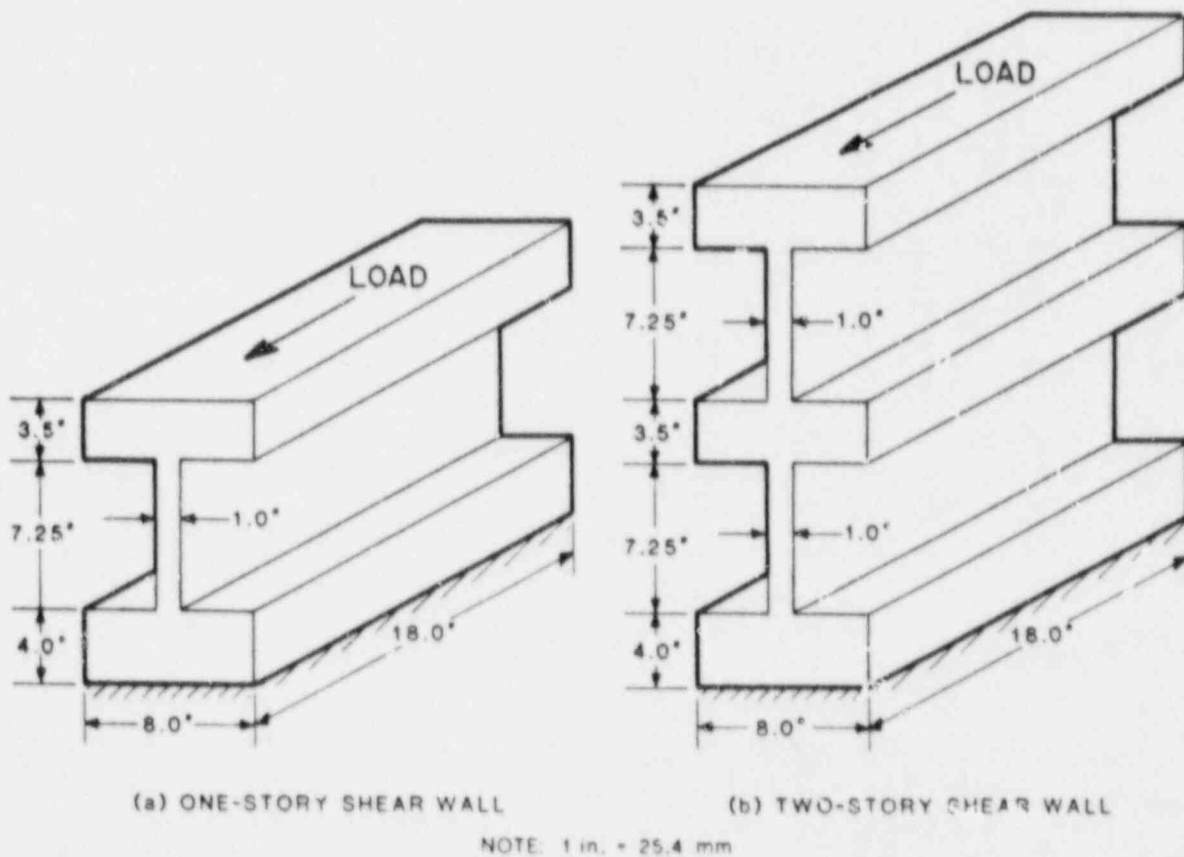
Fig. 1. One- and two-story shear wall elements.

north-south component of the 1940 El Centro earthquake. A detailed description
of the shear wall's geometry, material properties, testing program, and results
can be found in Ref. 1.

Next, one- and two-story, microconcrete, scale models of an idealized
diesel generator building were investigated. These structures were idealized
in the sense that the interior walls and penetrations in the exterior walls
that exist in the prototype were excluded to simplify the task of understand-
ing the model's structural response. The 1/30- and 1/10-scale two-story models
are shown in Fig. 2. A geometry that was identical to the second story of the
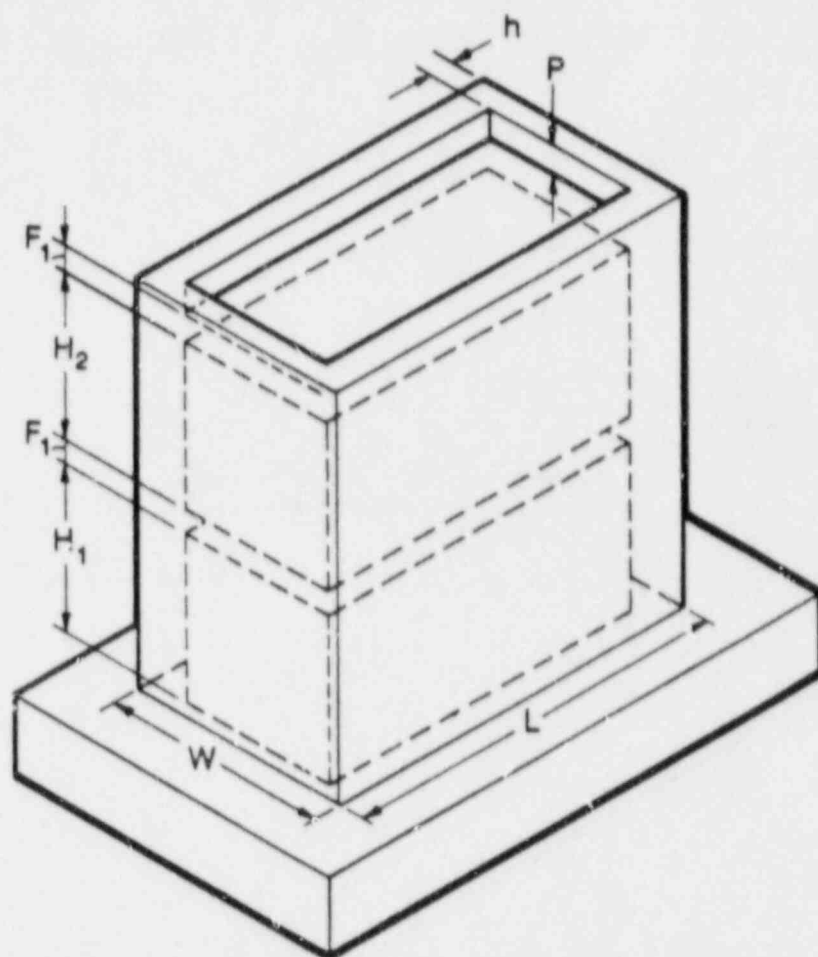
	h, F_1, F_2	W	L	H_1 & H_2	P	Wt/STORY *
1/30-SCALE	1 in.	10 in.	18 in.	7.25 in.	1 in.	47.7 lb
1/10-SCALE	3 in.	30 in.	54 in.	21.75 in.	3 in.	1286 lb
PROTOTYPE	30 in.	25 ft	45 ft	18.125 ft	30 in.	1,286,000 lb

*BASE NOT INCLUDED

NOTE: 1 in. = 25.4 mm, 1 ft = 0.305 m, 1 lb = 4.45 N

Fig. 2. Diesel generator building models.

1/30-scale two-story model was used for the one-story models. Static cyclic and monotonic loading was applied to the one-story models and both the one- and two-story models were subjected to random and simulated seismic base excitations. A summary of this testing can be found in Ref. 2.

The tests on the diesel-generator buildings were followed by tests on 1/42- and 1/14-scale, three-story, microconcrete models of an idealized auxiliary building. These structures are shown in Fig. 3. Random and simulated seismic base excitations were applied to both structures, and results of these tests are summarized in Ref. 3.

The last group of structures to be tested are referred to as the "TRG" structures. These structures consist of a shear wall bounded on either end by flexural boundary elements, as shown in Figs. 4-6. The acronym "TRG" comes
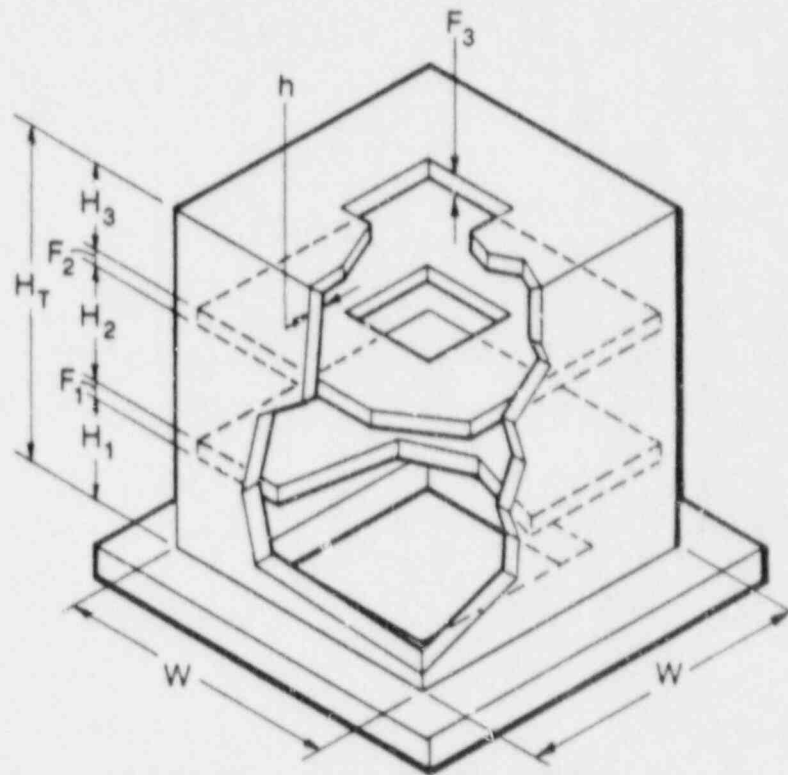
	h, F_1, F_2, F_3	W	H_1, H_2, H_3	Wt/STORY*
1/42-SCALE	1 in.	26 in.	10 in.	140 lb
1/14-SCALE	3 in.	78 in.	30 in.	3780 lb
PROTOTYPE	42 in.	1092 in.	420 in.	10,372,000 lb

* BASE NOT INCLUDED

NOTE: 1 in. = 25.4 mm, 1 lb = 4.45 N

Fig. 3. Auxiliary building models.

from the suggestion for this geometry by the Technical Review Group for this program. TRG-1, Fig. 4, was a microconcrete structure that was tested statically to low stress levels (80-psi maximum normal tensile stress) in a monotonic fashion. Also, for the purpose of performing an experimental modal analysis, TRG-1 was placed on a foam pad to simulate free boundary conditions and was excited in a uniaxial manner at one point by a small portable shaker (50-lb peak force) using a random input. TRG-1 was then put on a shake table and was subjected to random and simulated seismic base excitations. Similar tests were performed on TRG-3 (Fig. 5) except that a haversine pulse was used instead of the random base excitation and the static testing produced stresses that did not exceed a normal tensile stress of 40 psi (TRG-1 was a 1/4-scale
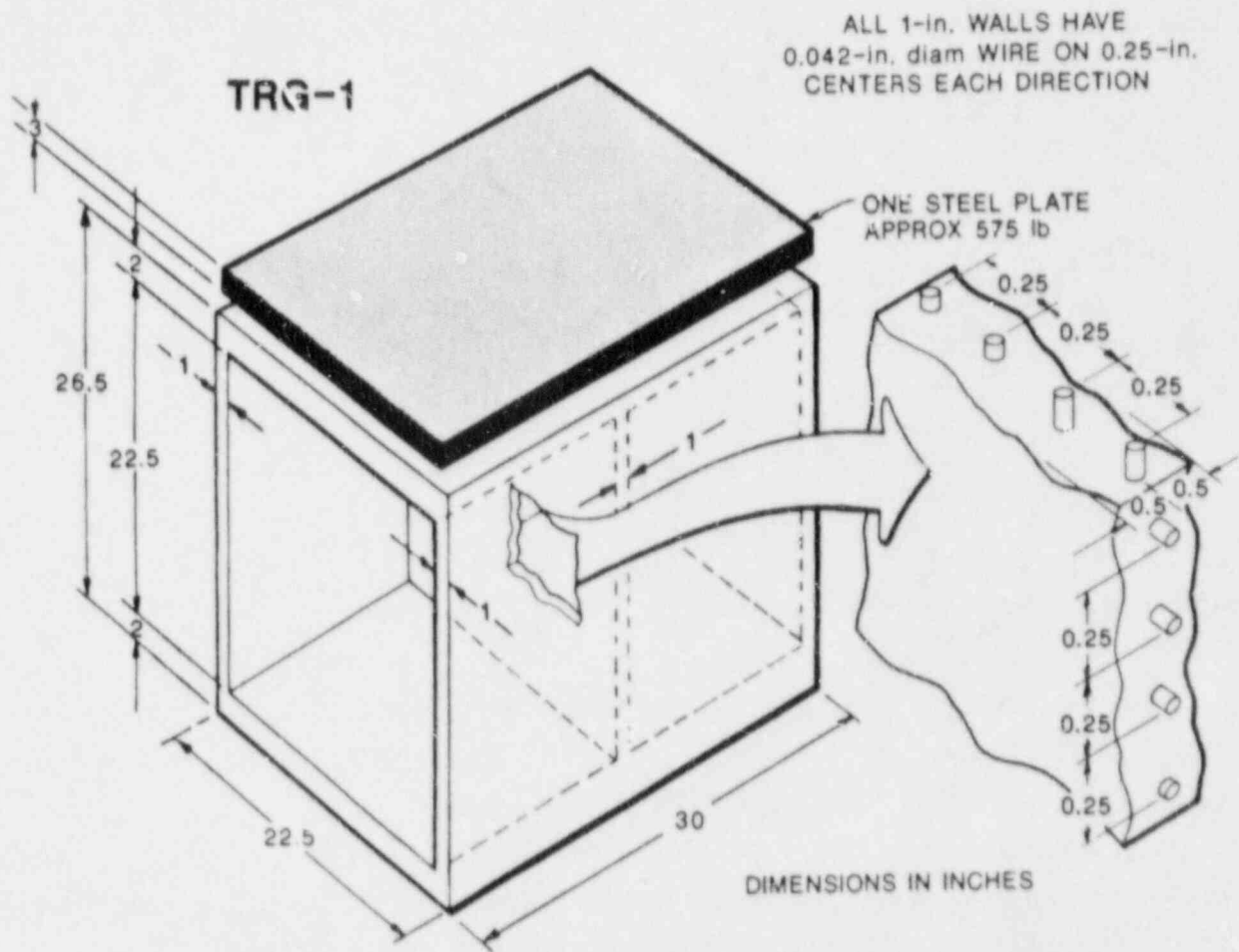
Fig. 4. 1/4-scale TRG type structure, TRG-1.

5

TRG-3, 5

ALL 4-in. WALLS HAVE No. 3
REBAR ON 4.5-in. CENTERS
EACH FACE, EACH DIRECTION

TWO STEEL PLATES
APPROX 18,800 lb EACH

STEEL PLATE
HELD IN PLACE BY
EIGHTEEN 1 1/4-in. BOLTS
TORQUED TO 400 ft.lb

DIMENSIONS IN INCHES
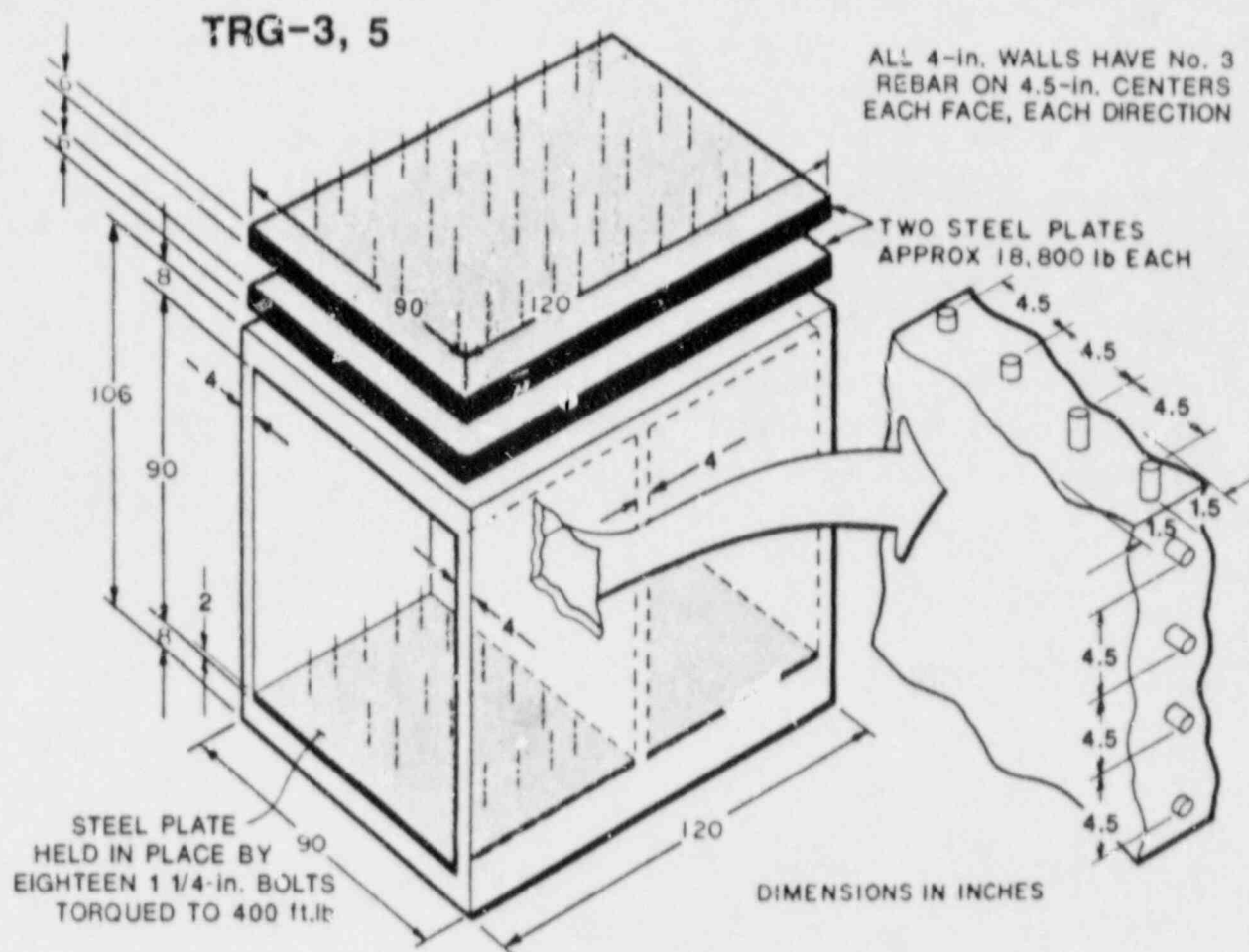
Fig. 5.   Four-inch-thick wall TRG type structure, TRG-3, 5.

model of the conventional concrete TRG-3 structure). A summary of the testing
performed on TRG-1 and TRG-3 can be found in Refs. 4 and 5, respectively.

TRG-4 and TRG-5, Figs. 5 and 6, were tested in a similar fashion. First,
an experimental modal analysis was performed with the structures resting on
air bearings to simulate free-boundary conditions. A 300-lb force shaker was
used to provide the uniaxial random input at a point for these tests. The
structures were then statically tested to failure in a cyclic manner. These
tests were followed by another experimental modal analysis of the structure in
its damaged state. A summary of this testing can be found in Ref. 6.

For all the structures that were tested on a shake table, random base
motion inputs were used to characterize the dynamic properties of the struc-
ture, and these excitations usually did not exceed 0.5-g peak acceleration.
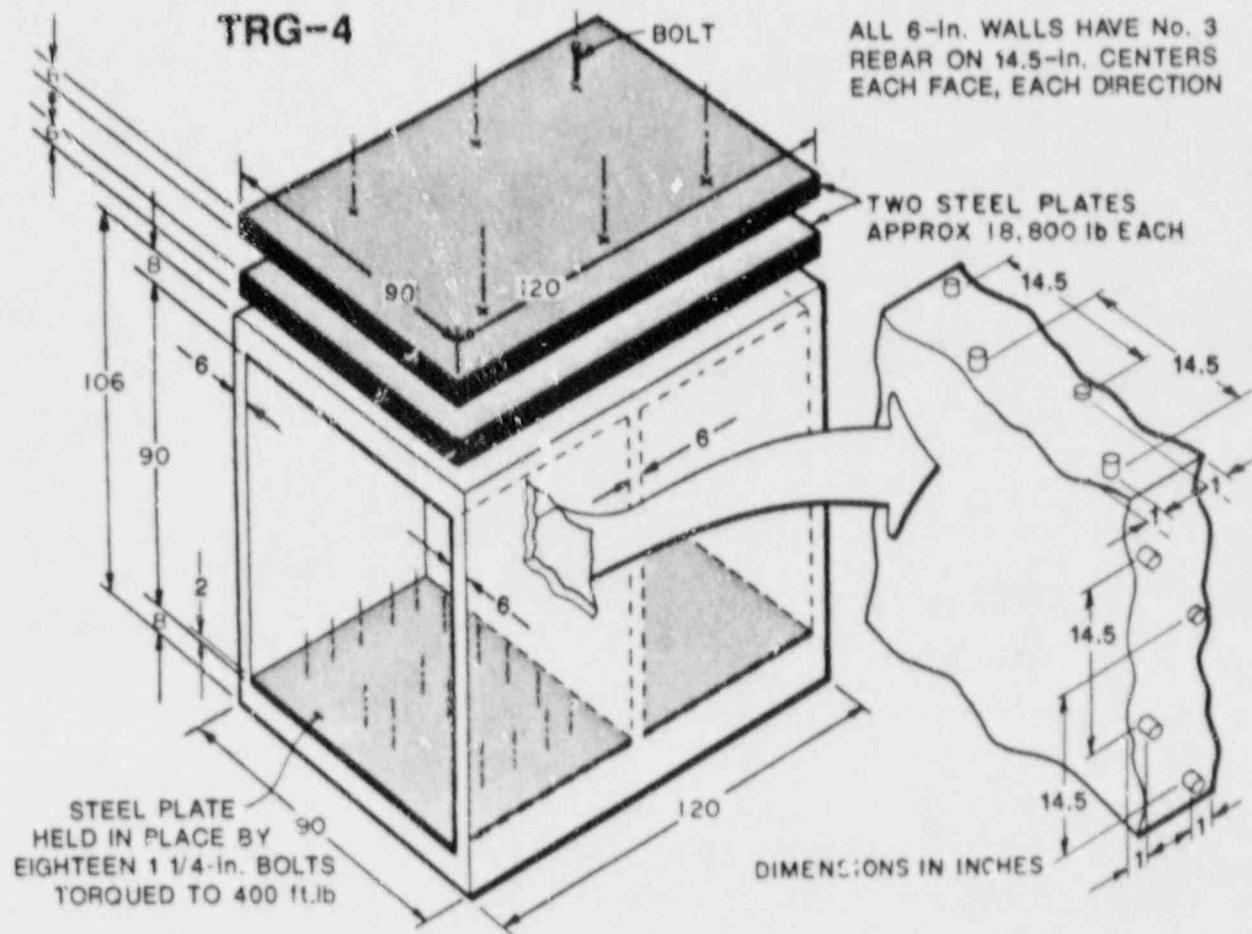
Fig. 6. Six-inch-thick wall TRG-type structure, TRG-4.

For TRG-3, a haversine pulse was used instead of a random signal, and, again, the peak acceleration was kept to a nominal value of 0.5 g. Most of the simulated seismic inputs began at a normal 0.5-g peak acceleration because this value was the lowest acceleration level for which the shake tables could be controlled. These inputs were progressively increased in the peak acceleration amplitude until the structure failed or until the shake table limits were reached.

A. General Discussion of Equations of Motion

The general equation of motion for an externally excited structural system is

$$\{F_m(t)\} + \{F_d(t)\} + \{F_k(t)\} = \{F(t)\} \quad , \tag{1}$$

where

    $\{F(t)\}$ = a vector of external forcing function,

    $\{F_m(t)\}$ = a vector describing the inertial force,

    $\{F_d(t)\}$ = a vector describing the damping force,

    $\{F_k(t)\}$ = a vector describing the restoring or spring force, and

    t   = time.

For a single degree-of-freedom system Eq. (1) takes the form

$$m\ddot{x}(t) + F_d(t) + kx(t) = F(t) \quad , \tag{2}$$

where

    m   = system mass,

    k   = structural stiffness,

    $\ddot{x}(t)$ = acceleration of the mass, and

    $x(t)$ = displacement of the mass.

The mass and stiffness properties of the structure can be derived explicitly from the structure's geometric and material properties. However, the damping characteristics must be inferred from test data on structures and structural elements.

For multi-degree-of-freedom systems, the equations of motion can be expressed as

$$[M]\{\ddot{x}(t)\} + \{F_d(t)\} + [k]\{x(t)\} = \{F(t)\} \quad , \tag{3}$$

where

    [M]   is an n x n mass matrix where n is the number
           of degrees-of-freedom in the system,

    $\{\ddot{x}(t)\}$ is an n x 1 acceleration vector,

    $\{F_d(t)\}$ is an n x 1 damping force vector,

    [k]   is an n x n stiffness matrix,

    $\{x(t)\}$ is an n x 1 displacement vector, and

    $\{F(t)\}$ is an n x 1 applied force vector.

Depending on the nature of the damping force vector, Eq. (3) can be un-coupled with standard modal analysis techniques.[7] In cases the damping forces are such that the equations of motion cannot be uncoupled, direct-time integration of the equations of motion is necessary to determine the response of the structure to a general forcing function.

B. Coulomb or Frictional Damping[8,9,10,11]

This type of damping results from the sliding of two dry surfaces on which damping force is assumed to be proportional to the normal force. The damping and normal forces are related to the kinetic coefficient of friction, μ, by the following equation

$$F_d = \mu N ,$$ (4)

where
F_d = damping force, and
N = normal force.

The kinetic coefficient of friction is usually less than the static coefficient of friction, and the kinetic coefficient is assumed to be independent of displacement and frequency. Because of this independence, the Coulomb damping force is essentially constant throughout the response of the structure, and changes in the coefficient of friction as the structure cycles through a zero velocity point are assumed to be negligible. Coulomb damping is nonlinear with a discontinuity in the damping force occurring whenever there is a change in the direction of relative velocity. The equation of motion for a single degree-of-freedom system with Coulomb damping is

$$m\ddot{x}(t) + F_d \, \text{sgn} \{\dot{x}(t)\} + kx(t) = F(t) ,$$ (5)

where
$\dot{x}(t)$ = velocity of the mass, and sgn denotes the signum function.

From Eq. (5) it can be shown that, for free-vibration response, the structure will vibrate with a frequency $\omega = \sqrt{k/m}$ and that the peak amplitudes of the response will decay in a linear manner. Motion will stop when displacements

are such that the restoring force of the spring is insufficient to overcome the static friction force.

C. Hysteretic Damping[7,8,11]

Materials that are not perfectly elastic exhibit energy losses due to their internal damping properties. This type of damping is assumed to be proportional to displacements and in phase with velocity and is defined by the following equation:

$$f_d = \frac{\pi}{2} h |x(t)| \frac{\dot{x}(t)}{|\dot{x}(t)|} ,$$

(6)

where

h = hysteretic damping coefficient.

For a single-degree-of-freedom system, the hysteretic damping is described approximately by a viscous damping force that varies inversely with the frequency of vibration such that the damping force is independent of frequency. The hysteretic energy loss per cycle is

$$W_o = \pi h A^2 ,$$

(7)

where

W_o = energy loss per cycle,
A = amplitude of peak response.

This expression can be equated to the energy loss per cycle, W_D, due to a viscous damper given by

$$W_D = C\pi\omega A^2 ,$$

(8)

and an equivalent viscous damping coefficient, $C_{Eq} = (h/\omega)$, is obtained. The equation of motion becomes

$$m\ddot{x}(t) + \frac{h}{\omega} \dot{x}(t) + kx(t) = F(t) .$$

(9)

10

If F(t) is limited to a harmonic function, this equation may be readily solved. When the input signal is harmonic, hysteretically damped systems can be modeled with a complex stiffness term

$$k^* = k(1 + i\eta) , \tag{10}$$

where
k^* = complex stiffness,
$i = \sqrt{-1}$,
η = loss factor = $\frac{h}{k}$,

and the equation of motion becomes

$$m\ddot{x}(t) + k(1 + i\eta) x(t) = F(t) . \tag{11}$$

In some texts,[7,8,9] the term hysteretic damping is used interchangeably with structural damping. However, other references[12] refer to structural damping as the combination of hysteretic damping and other damping mechanisms, such as Coulomb and velocity-squared damping.

D. Viscous Damping[7-11]

A viscous damping mechanism is obtained when a system vibrates in a fluid. The viscous damping force is proportional to velocity and can be expressed as

$$F_d = C\dot{x}(t) , \tag{12}$$

where
C = viscous damping coefficient.

This damping mechanism is the most common form used in the analysis of structures because it leads to a linear differential equation of motion of the form

$$m\ddot{x}(t) + C\dot{x}(t) + kx(t) = F(t) . \tag{13}$$

Most test evidence shows that the damping forces in structures are frequency independent. A viscous damping mechanism contradicts these experimental

findings; hence, this mechanism is not representative of the actual energy dissipation mechanism in most structural systems. However, an equivalent viscous damping mechanism can be determined for nonviscously damped systems by equating the energy loss per cycle from the actual damping mechanism to the energy loss per cycle in a similar viscously damped system when the system has steady-state harmonic response. This allows the mathematical convenience of the viscous damping mechanism to be extended to other nonlinear damping mechanisms. Reference 7 summarizes the equivalent viscous damping expressions for various damping mechanisms.

The popularity of viscous damping for modeling damping mechanisms in multi-degree-of-freedom vibrating solids is purely because of mathematical convenience. The undamped equations of motion for a structural system are

$$[M]\{\ddot{x}\} + [K]\{x\} = \{F(t)\} \quad . \tag{14}$$

Coordinates that uncouple these equations of motion (i.e., make [M] and [K] diagonal matrices) are called "normal" coordinates. The solution to Eq. (14) for a general forcing vector $\{F(t)\}$ is readily obtained by transforming the equations to uncouple them, integrating the uncoupled equation, and transforming the solution back into the original coordinates (the normal mode method). The presence of the damping terms, $[C]\{\dot{x}\}$, makes it natural to ask if [C] can be diagonalized also. There is a general method for uncoupling Eq. (3), but it means solving an eigensystem that is 2n x 2n in size as opposed to an n x n system (see Ref. 13), and, thus, this method is not generally used. However, it is clear that if [C] is proportional to either [M] or [K] or to a linear combination of [M] and [K], then Eq. (3) expressed in normal coordinates will be uncoupled and in the form of

$$m\ddot{q} + c\dot{q} + kq = F(t) \quad , \tag{15}$$

where

$$\{x\} = [\Phi]\{q\} \quad , \tag{16}$$

with [Φ] being the normal mode matrix of eigenvalues. Each of the uncoupled equations (15) can be integrated and the back transformation given by Eq. (16)

12

can be used to obtain the response vector {x}, thus preserving the normal mode solution method.

It is also clear that, in dealing with the uncoupled equations, all the traditional methods for finding the maximum response of a single-degree-of-freedom model can be used if a rule or rules for combining these responses can be formulated. These methods are the response spectra methods and their associated rules for combining the individual modal maxima. The point is, even though there is little evidence for viscous damping mechanisms in vibrating structures, the mathematical convenience of solving for the modal responses by the normal mode method is very appealing and has led to a large body of literature in this area.

Damping using $[C] = \alpha[M]$ or $\alpha[K]$, as discussed above, is commonly called "proportional" damping. Damping for which $[C] = \alpha_1[M] + \alpha_2[K]$ is commonly called "Rayleigh" damping.

One further point about viscous damping in concrete structures can be made. It is shown (Ref. 14), that, if the damping mechanism is viscous in nature, there is a scaling relationship between two differently sized, but scale-model structures. By scale model, we mean that the laws of similitude are satisfied. One of the structures can be considered the prototype. In fact, it is shown that, for the types of models tested in the Seismic Category I Structures Program, the viscous damping ratios for a 1/30-scale model of a diesel generator building and a 1/10-scale model will vary as

$$\frac{\zeta_{1/10}}{\zeta_{1/30}} = 1/3 \quad . \tag{17}$$

where $\zeta = C/C_c$,

and $C_c = 2\sqrt{km}$ is the critical damping value.

However, measured damping ratios for these models, are discussed in a later section, indicate that, up to very large values of applied base seismic input (1 g on a prototype Cat. I diesel generator building), the damping is essentially constant and independent of scale. Thus, it has been concluded the physical damping mechanism in concrete is not viscous in nature.

13

II. EXPERIMENTAL METHODS

Experimentally, there are four basic methods we have used for quantifying
damping. These methods are (1) the frequency response function method, (2)
response spectra matching method, (3) the log decrement method and, (4) the
hysteretic energy loss method. These methods will be discussed in the
following sections.

A. Influence of the Types of Loading

The experimental methods used to determine damping properties of a struc-
ture are, in some cases, applicable with only certain types of loading. As
long as a structure remains linear, the frequency response function method
will be independent of the type of dynamic excitation used. This method does
require the measurement of input excitations as well as the structure's
response. This method is valid when used with either force or acceleration
inputs. If the structure is responding in the nonlinear range, the frequency
response function will depend on the amplitude and frequency content of the
input, and, hence, the damping identified by this method would be specific to
the input signal.

The respons. spectra matching method is also independent of the type of
loading used to excite the structure. This method is not restricted to the
analysis of linear response data, but it is restricted by the structural
model's ability to predict nonlinear response. Again, this method requires
the input excitations to be measured along with the structures response, and
the method is equally valid for base excitations or for force inputs.

The log decrement method is based on measurement of the free-vibration
response of an under-damped structure. Only the free vibration response of
the structure is measured. It is unnecessary to measure or know the nature of
the force required to initiate the free vibration. Although there are no
limitations on the types of forces required to induce the vibration, the most
practical means of initiating the free vibration is either a "pluck" test or a
dynamic impulsive load.

Measurements of hysteretic energy loss require that a static, cyclic load
be applied to and measured on the structure. The loads must be of sufficient
magnitude so that accurate displacement measurements can be obtained.

14

B. Frequency Response Function Method

For the structures tnat were tested in the program absolute acceleration response, absolute acce'eration input, frequency response functions were measured. This frequency response function is defined as the Fourier transform of the absolute acceleration response divided by the Fourier transform of the acceleration input at the base of the structure. This function is complex and, for a single degree-of-freedom, base-excited structure, the real portion of the frequency response function can be expressed as

$$H(f)_{real} = \frac{1 - \left(\frac{f}{f_n}\right)^2 + 2\zeta\left(\frac{f}{f_n}\right)^2}{\left\{1 - \left(\frac{f}{f_n}\right)^2\right\}^2 + 2\zeta\left(\frac{f}{f_n}\right)^2} , \tag{18}$$

where

$H(f)$ = frequency response function,

f = frequency in cycles/s,

f_n = the structure's natural frequency, and

ζ = equivalent viscous damping ratio.

A typical plot of the real portion of a frequency response function is shown in Fig. 7. When Eq. (18) is analyzed to determine the maximum and minimum points in the real portion of the frequency response function, the equivalent viscous damping ratio can be determined from the following expression

$$\zeta = \frac{1}{2}\left[\frac{\left(f_{min}/f_{max}\right)^2 + 1}{\left(f_{min}/f_{max}\right)^2 - 1}\right] . \tag{19}$$

As long as the structure remains linear, this method for evaluating damping is independent of the excitation force. The method assumes that the structure's response can be accurately described by a linear second-order differential equation of the form in Eq. (13). For multi-degree-of-freedom systems, it is also assumed that there is little modal coupling and that the structure is behaving as a single-degree-of-freedom around its resonant frequency. In this

15
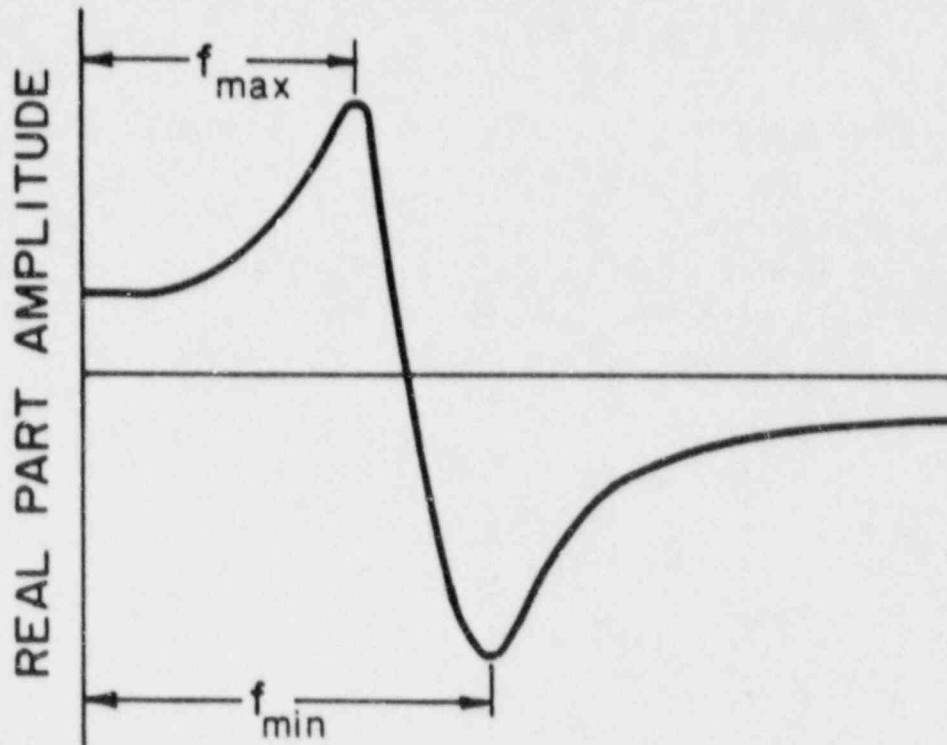
Fig. 7. Estimation of equivalent viscous
damping from the real part of the
frequency response function.

case, the method can be used to evaluate the viscous damping associated with
each mode of vibration. Other methods, described in Ref. 15 can be applied to
frequency response functions data when there is significant modal coupling.

This method is appropriate when a reinforced concrete structure has been
damaged because the structures have been shown to respond in a linear fashion
with a reduced stiffness after cracking. Even during simulated seismic trans-
ients that introduce additional cracking, the damage is introduced during the
initial cycles of the excitation and the majority of the response is again
linear with a further reduced stiffness.

C. Log Decrement Method

The log decrement method determines an equivalent viscous damping ratio
from the decay in peak amplitudes during free vibration response. For a vis-
cously damped, single-degree-of-freedom system, the amplitude of response is

$$x(t) = \rho \, e^{-\zeta\omega t} \cos(\omega_d t - \theta) \quad , \qquad\qquad (20)$$

16

where

$$\rho = \left\{ \left[\frac{\dot{x}(o) + x(o)\zeta\omega}{\omega_d} \right]^2 + \left[x(o) \right]^2 \right\}^{1/2} .$$ (21)

$$\theta = \tan^{-1} \left[\frac{\dot{x}(o) + x(o)\zeta\omega}{\omega_d \, x(o)} \right] ,$$ (22)

$\dot{x}(o)$ = initial velocity,

$x(o)$ = initial displacement, and

ω_d = damped natural frequency = $\omega\sqrt{1-\zeta^2}$.

The ratio of two positive peaks m cycles apart is

$$\frac{x_n}{x_{n+m}} = \exp\left(2\pi m\zeta\frac{\omega}{\omega_d} \right).$$ (23)

The logarithmic decrement, δ, is defined as

$$\delta = \ln\left(\frac{x_n}{x_{n+m}} \right) = 2\pi m\zeta \frac{\omega}{\omega_d} ,$$ (24)

and this quality can be approximated as

$\delta \approx 2\pi m\zeta$, for lightly damped systems.

A series expansion of the ratio of the positive peaks yields

$$\frac{x_n}{x_{n+m}} = e^{\zeta} \approx e^{2\pi m\zeta} = 1 + 2\pi m\zeta + \frac{(2\pi m\zeta)^2}{2} + \dots$$ (25)

By neglecting higher-order terms in ζ, the following approximation can be obtained for the equivalent viscous damping ratio based on two positive peak responses m cycles apart:

$$\zeta \stackrel{\approx}{=} \frac{x_n - x_{n+m}}{2\pi m \, x_{n+m}} \tag{26}$$

A similar relationship may be obtained for positive peak acceleration responses. Correction factors for the approximate expression in this equation can be found in Ref. 11.

This method assumes that the structure is behaving as a linear single-degree-of-freedom system and that the free vibration response can be represented by a linear differential equation of the form in Eq. (13).

If the mechanism for energy dissipation is Coulomb damping, the decay in the positive peak responses will be linear, and, from work-energy principles, the frictional damping force can be estimated as

$$F_d = \frac{k\{x_1(t) - x_2(t)\}}{4} \tag{27}$$

where

$x_1(t)$ = positive peak displacement, and

$x_2(t)$ = subsequent positive peak displacement.

This expression also assumes that the structure is behaving as a single-degree-of-freedom system and that the stiffness of the system is not changing during the free vibration response.

D. Floor Response Spectra (FRS) Matching Method

The floor response spectra matching method is a technique in which stiffness and damping of a test specimen are estimated from comparisons of FRS determined from analytical models (analytical FRS) with FRS generated from experimentally measured acceleration-time histories (measured FRS).

The FRS matching method consists of the following steps:

1. A simple, lumped mass analytical model is developed with a transnational degree-of-freedom associated with each floor level. This type of model is shown in Fig. 8 for a two-story diesel generator building.

18

2. Lumped masses are assigned to each degree-of-freedom based on the mass of the floor slab, the external masses attached at a floor level to satisfy similitude requirements, and empirical methods for lumping the distributed mass of the wall to a floor level.

3. Stiffness values are assigned to each floor. In this work, because of the geometry of the multi-story test structures, the same stiffness value was usually assigned to all floors. The initial estimate of the stiffness value, K, was based on the theoretical stiffness value determined from strength-of-materials principles, K_t, assuming an uncracked section and also assuming that end walls were fully effective. (This stiffness value was then weighted by the square of the ratio of the measured fundamental frequency, f_m, to the theoretical fundamental frequency, f_t, determined using the theoretical stiffness so that

$$K = K_t \left(\frac{f_m}{f_t} \right)^2 \quad . \tag{28}$$

4. Viscous damping ratios are assigned to each degree-of-freedom. In most cases, an initial estimate of 7% of critical was used. Again, for multi-degree-of-freedom systems, the same damping ratio was assigned to each degree-of-freedom. The resulting equation of motion is

$$[M]\{\ddot{x}\} + [C]\{\dot{x}\} + [K]\{x\} = -[M]\{\ddot{y}\} \tag{29}$$

where C & M are diagonal, x is the relative displacement vector, and $\{\ddot{y}\}$ is the absolute base acceleration vector.

5. With the parameters determined in Steps 2-4, the analytical model was driven with the actual acceleration-time signal to which the structure was subjected during a test. This step requires that, for the test chosen, the actual base input acceleration-time signal must be digitized for use in the analytical solution. For a particular base input, the equations of motion were numerically integrated using a fourth-order Runge-kutta scheme to determine the acceleration response at each degree-of-freedom.

6. The analytically determined acceleration-time histories were then used to calculate floor response spectra, and these FRS were compared with the measured FRS.

7. Steps 3-6 were repeated until the analytical FRS matches the measured FRS.

This method can easily incorporate other damping mechanisms or combinations of damping mechanisms into the matching process. However, at this point,
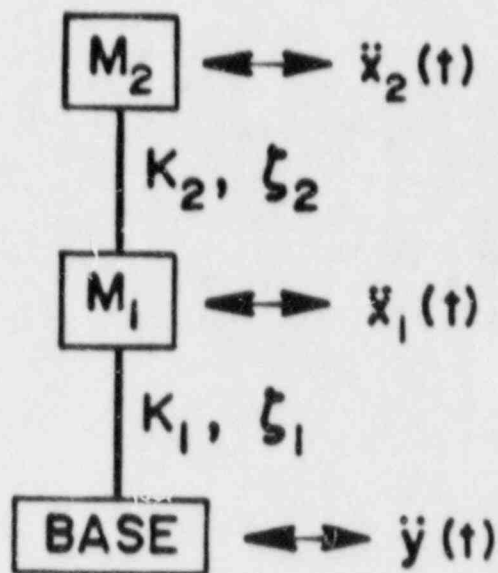
Fig. 8. Lumped mass model used to analyze a two-
story diesel generator building model.

only viscous damping has been investigated. The use of this method was first
reported in Ref. 2 and was stated to have limited success. Further refinement
in the method and refinement in the digitizing of the experimental data have
shown that the analytical models can match the measured FRS, even when the
test specimens have been severely damaged.

This method can give erroneous values for damping if there is significant
noise in the measured acceleration-time histories. Also, it is not clear that
there is a unique set of damping and stiffness coefficients that will produce
a best comparison between the measured and analytical FRS. Finally, for multi-
degree-of-freedom systems, the model that best matches the top floor response
generally over-predicts the bottom floor response.

E. Hysteretic Energy Loss Method

The energy loss that occurs during a static, cyclic test of a specimen
can be used to obtain an equivalent viscous damping ratio. This is done by
equating the hysteretic energy loss measured during the static test to the
energy dissipated by viscous damping in a linear single-degree-of-freedom

system during steady-state response to one cycle of harmonic forced excitation.
From Reference 9, the energy lost due to viscous damping, W_{VD}, is

$$W_{VD} = \pi C A^2 \omega \quad . \tag{30}$$

where

A   = amplitude of steady-state vibration,

ω = frequency of steady-state vibration, and

the hysteretic energy loss, W_H is defined as

$$W_H = H, \tag{31}$$

where

H   = area within the hysteresis loop.

Equating (30) and (31) yields

$$C = \frac{H}{\pi A^2 \omega} \quad . \tag{32}$$

For a single-degree-of-freedom system, the critical damping coefficient is defined as

$$C_c = 2 \sqrt{Km} \quad . \tag{33}$$

Dividing both sides of (32) by C_c yields

$$\frac{C}{C_c} = \frac{H}{2\pi A^2 \omega \sqrt{Km}} \quad . \tag{34}$$

As stated in Ref. 9, the most significant influence of damping occurs around the resonant frequency and, for a SDOF system, that frequency can be expressed as

$$\omega = \sqrt{\frac{k}{m}} \quad . \tag{35}$$

Substituting (35) into (34) yields the expression that relates the equivalent viscous damping ratio to the static hysteretic energy loss.

$$\frac{C}{C_c} = \frac{H}{2\pi A^2 k} \quad . \tag{36}$$

This method is dependent on the stiffness being well defined and constant for the entire load cycle.

III. EXAMPLES OF EXPERIMENTAL ASSESSMENT OF DAMPING

A. Frequency Response Function Method

The real part of a frequency response function, measured on a 1/30-scale, single-story diesel generator building model, is shown in Fig. 9. For this case, f_{min} = 69.3 Hz, f_{max} = 61.5 Hz, and the equivalent viscous damping ratio is

$$z = \frac{1}{2} \left[\frac{\left(\frac{69.3}{61.5}\right)^2 + 1}{\left(\frac{69.3}{61.5}\right)^2 - 1} \right] = 4.2\% \quad . \tag{37}$$
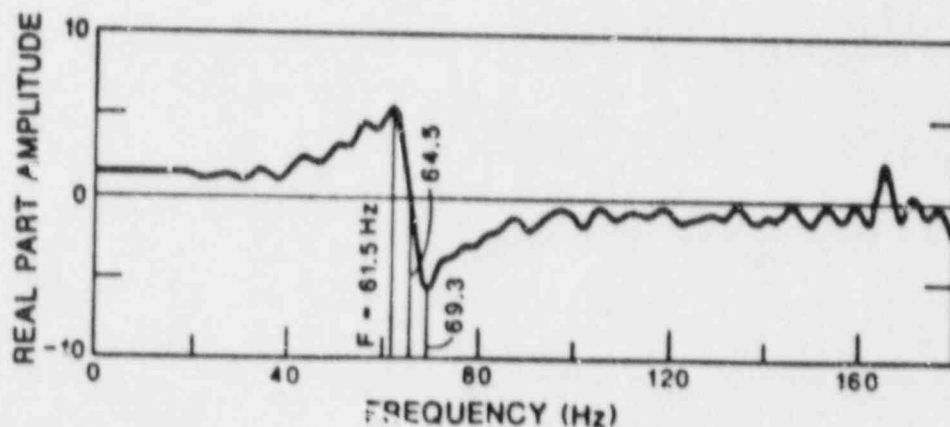
Fig. 9. The real part of a measured frequency response function from a 1/30-scale diesel generator building model.

22

B. Log Decrement Method

The acceleration-time response of TRG-3 to a 0.9-nominal-peak-acceleration haversine pulse is shown in Fig. 10. Using the first and second peaks, the equivalent viscous damping ratio is

$$\zeta \approx \frac{(0.58g - 0.48g)}{2\pi \, 0.48g} = 3.3\% \quad . \tag{38}$$

A variety of damping values can be obtained from this plot because any combination of peaks in the response can be used. An analysis of all possible combinations of peak positive amplitudes for this case yields damping ratios that range from 3.3% to 16%, with an average value of 9.8%. The scatter in this data was caused by continued input into the system after the haversine pulse was to have stopped.
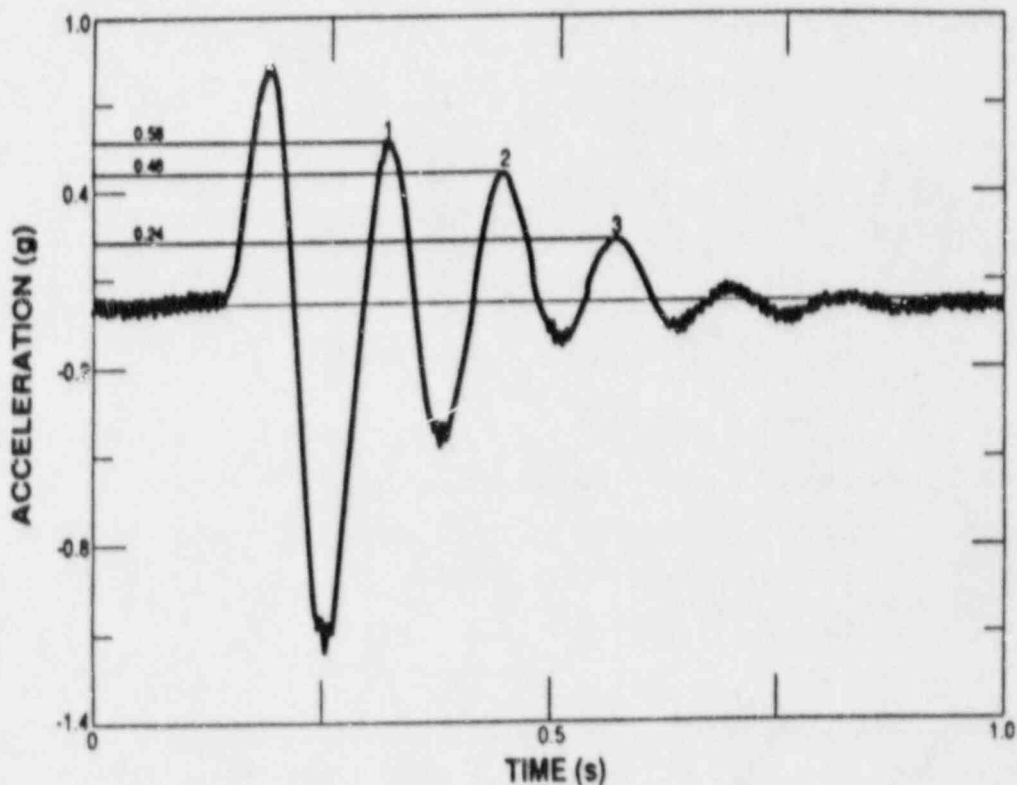
Fig. 10. Free vibration response of the TRG-3
structure subjected to a Haversine pulse.

C. Floor Response Spectra Matching Method

Figure 11 shows the floor response spectra calculated from measured acceleration-time response of the top slab on the TRG-3 structure for a 1.6-g simulated seismic input. Also shown in this figure is the floor response spectra generated for the same location with acceleration-time data from a single-degree-of-freedom analytical model of the TRG-3 structure. The analytical model, shown in Fig. 12, was driven with a digitized form of the measured base excitation used in the experiment. To obtain this match, a viscous damping ratio of 8.5% was used in the analysis.

D. Hysteresis Method

Figure 13 shows the static load-deflection curve for one cycle of loading performed on the TRG-4 structure. The area within the curve represents the hysteretic energy loss. For this particular cycle, the hysteretic energy loss was 29.5 in.-lb. The stiffness for this cycle was measured as 9.48×10^6 lb/in., and the peak amplitude of displacement was 2.7×10^{-3} in. From this data, the equivalent viscous damping ratio was

$$\zeta = \frac{29.5 \text{ in.-lb} \times 100}{2\pi (2.7 \times 10^{-3} \text{ in.})^2 \, 9.48 \times 10^6 \text{ lb/in.}} = 6.8\% \quad . \tag{39}$$

IV. SUMMARY OF EXPERIMENTAL RESULTS

Tables I-IV summarize the equivalent viscous damping ratios that were determined from measured hysteretic energy losses during static cyclic testing. Results from isolated microconcrete shear walls[1] are listed in Tables I-II, and results from the cyclic tests on the TRG type[6] structures are summarized in Tables III-IV.

The log decrement method was used only with data from the TRG-3 structure[5] when that structure was subjected to a haversine pulse. Figure 10 shows the horizontal acceleration response of the top slab of the TRG-3 structure. The possible equivalent viscous damping ratios that can be identified from the various combinations of peak response are summarized in Table V. Data from the first two peaks were not used because the shake table was continuing to input motion during this time and the log decrement method assumes that the structure is responding in a free vibration manner.

24
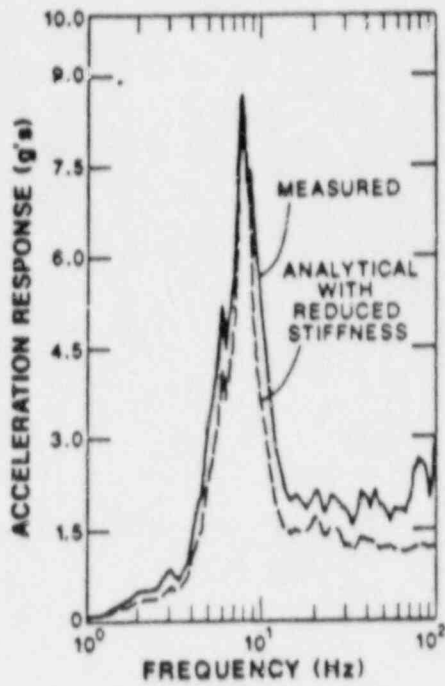
Fig. 11. Comparison of measured and calculated floor response spectra for TRC-3.

SINGLE-DEGREE-OF-FREEDOM IDEALIZATION OF THE TRG-3 STRUCTURE
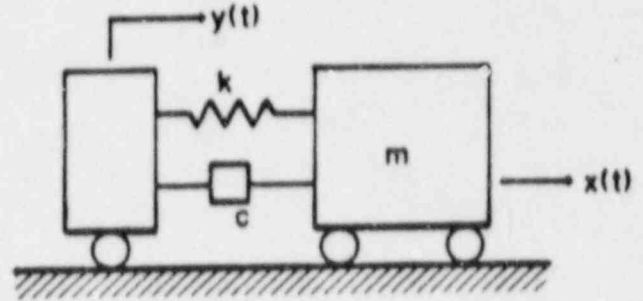
Fig. 12. Lumped mass model used to analyze TRG-3.

FIRST 50-PSI LOAD CYCLE — TRG4

H, THE AREA REPRESENTING THE HYSTERETIC ENERGY LOSS

$C/C_{cr} = H/2\pi A^2 K$

$K = \Delta F/\Delta D$
$A = \Delta D/2$

THE STRAIGHT LINE THAT THE COMPUTER PROGRAM CONSTRUCTS BETWEEN THE TERMINAL AND INITIAL DATA POINTS
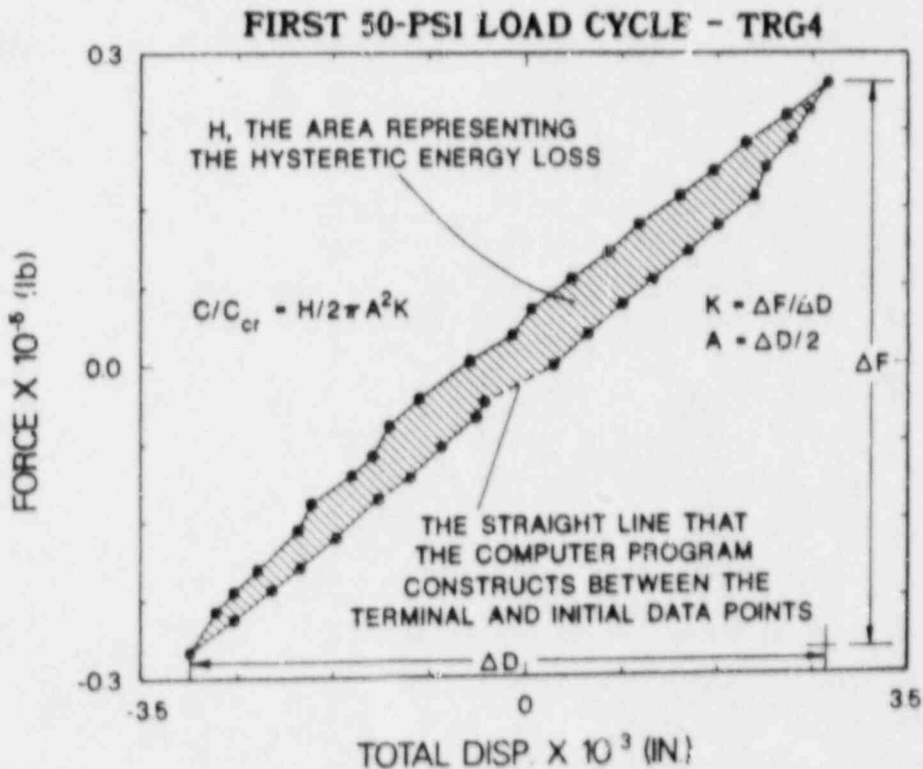
Fig. 13. Load-deformation response of TRG-4.

TABLE I

HYSTERETIC ENERGY LOSSES MEASURED ON ISOLATED SHEAR WALL SPECIMEN 3

Load Cycle	Peak Force (lb)	Hysteretic Energy Loss (in.-lb)	Equivalent Viscous Damping (% of Critical)
7	3000	3	5.8
11	4240	10	6.8
14	4920	21	9.0
19	4920	23	9.4
26	5920	62	8.7
28	5920	68	7.7

TABLE II

HYSTERETIC ENERGY LOSSES MEASURED ON ISOLATED SHEAR WALL SPECIMEN 5

Load Cycle	Peak Force (lb)	Hysteretic Energy Loss (in.-lb)	Equivalent Viscous Damping (% of Critical)
7	2740	2	5.0
10	3880	7	6.4
13	4040	18	8.9
15	4960	40	10.9
16	5600	126	21.7
17	5880	173	18.3

TABLE III

HYSTERETIC ENERGY LOSSES MEASURED ON TRG-4

Load Cycle	Peak Force (lb)	Hysteretic Energy Loss (in.-lb)	Equivalent Viscous Damping (% of Critical)
1	27000	29	5.9
2	27000	35	7.0
3	54000	113	5.2
4	54000	81	3.7
5	54000	77	3.5
6	108000	1560	*
7	108000	940	5.7
8	108000	888	4.9
9	140400	16400	*
10	27000	582	6.3

---

* Cycles that exhibited nonlinear response. Stiffness was not well defined during these cycles.

TABLE IV

HYSTERETIC ENERGY LOSSES MEASURED ON TRG-5

Load Cycle	Peak Force (lb)	Hysteretic Energy Loss (in.-lb)	Equivalent Viscous Damping (% of Critical)
1	18000	10	3.5
2	18000	10	3.4
3	18000	11	4.0
4	26000	39	3.3
5	36000	33	2.7
6	36000	32	2.8
7	54000	156	*
8	72000	786	*
9	72000	475	3.8
10	72000	449	3.5
11	108000	2630	*
12	108000	1690	4.6
13	108000	1300	3.4
14	144000	12000	*
15	180000	11300	*
16	18000	434	*
17	18000	293	8.0

*   Cycles that exhibited nonlinear response. Stiffness was not well defined during these cycles.

TABLE V

EQUIVALENT VISCOUS DAMPING RATIOS FOR THE TRG-3 STRUCTURE IDENTIFIED FROM FREE VIBRATION LOG DECREMENT DATA

Peak*	Equivalent Viscous Damping (% of Critical)
1-2	3.3
2-3	16.
1-3	11.

*   See Fig. 9.

The floor response spectra matching method was applied to TRG-1, [4] TRG-3, [5] a two-story, 1/10-scale diesel generator building model (CERL1), [2] and a three-story 1/42-scale auxiliary building model (SANDIA). [3] An analytical model similar to the one shown in Fig. 12 was used for both TRG-1 and TRG-3. Figure 8 shows the analytical model used for the CERL1 structure. Figure 14 shows the analytical model that was used with the SANDIA structure. Only a translation degree-of-freedom was assigned at each floor level. The damping ratios that provided the best fit of the analytical response to the calculated response are summarized in Tables VI-IX.
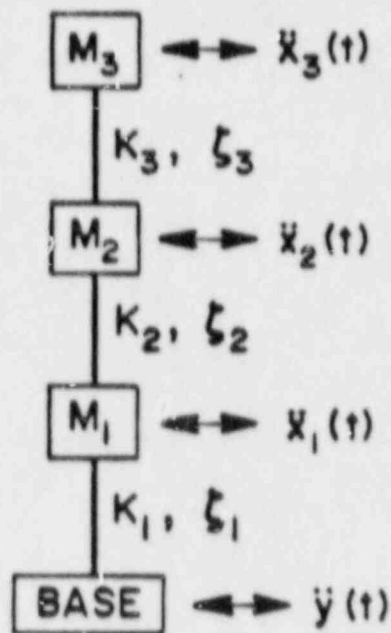
Fig. 14. Lumped mass model
used to analyze a
three-story auxiliary
building model.

TABLE VI

EQUIVALENT VISCOUS DAMPING RATIOS THAT WERE USED
WITH THE RESPONSE SPECTRA MATCHING TECHNIQUE FOR
FOR THE ANALYSIS OF TRG-1

Excitation Level* (g's)	Equivalent Viscous Damping (% of Critical)
0.21	7
2.54	22
7.23	13

* Peak acceleration base input from the time-scaled
version of the 1940 El Centro earthquake.

The real part of the frequency response function was used to determine
viscous damping ratios for diesel generator building models,[2] the auxiliary
building models,[3] and the TRG-1[4] and TRG-3[5] structures. Results
from the tests on the diesel generator buildings are shown in Fig. 15. These
results show the scale effects on the viscous damping ratio as identified by
the frequency response function analysis method. From this figure, it is evi-
dent that the scale effects, if any, are within the scatter of the data.

28

TABLE VII

EQUIVALENT VISCOUS DAMPING RATIOS THAT WERE USED WITH THE RESPONSE SPECTRA MATCHING TECHNIQUE FOR THE ANALYSIS OF TRG-3

Excitation Level* (g's)	Equivalent Viscous Damping (% of Critical)
0.88	8.5
0.99	8.5
1.65	8.5

* Peak acceleration base input from the time-scaled version of the 1940 El Centro earthquake.

TABLE VIII

EQUIVALENT VISCOUS DAMPING RATIOS THAT WERE USED WITH THE RESPONSE SPECTRA MATCHING TECHNIQUE FOR THE ANALYSIS OF CERL1

Excitation Level* (g's)	Equivalent Viscous Damping** (% of Critical)
1.88	$\zeta_1 = \zeta_2 = 6.0$
3.53	$\zeta_1 = 15, \zeta_2 = 11$
13.60	$\zeta_1 = 35, \zeta_2 = 10$

* Peak acceleration base input from a time-scaled version of the 1940 El Centro earthquake.
** See Fig. 8 for the degrees-of-freedom associated with ζ_1 and ζ_2.

TABLE IX

EQUIVALENT VISCOUS DAMPING RATIOS THAT WERE USED WITH THE RESPONSE SPECTRA MATCHING TECHNIQUE FOR THE ANALYSIS OF SANDIA

Excitation Level* (g's)	Equivalent Viscous Damping** (% of Critical)
0.65	$\zeta_1 = 12$ $\zeta_2 = 7$ $\zeta_3 = 4$
1.27	$\zeta_1 = 8$ $\zeta_2 = 7$ $\zeta_6 = 6$
2.83	$\zeta_1 = 15$ $\zeta_2 = 14$ $\zeta_3 = 13$

* Peak acceleration base input from a time-scaled version of the 1940 El Centro earthquake.
** See Fig. 14 for the degrees-of-freedom associated with ζ_1, ζ_2, and ζ_3.
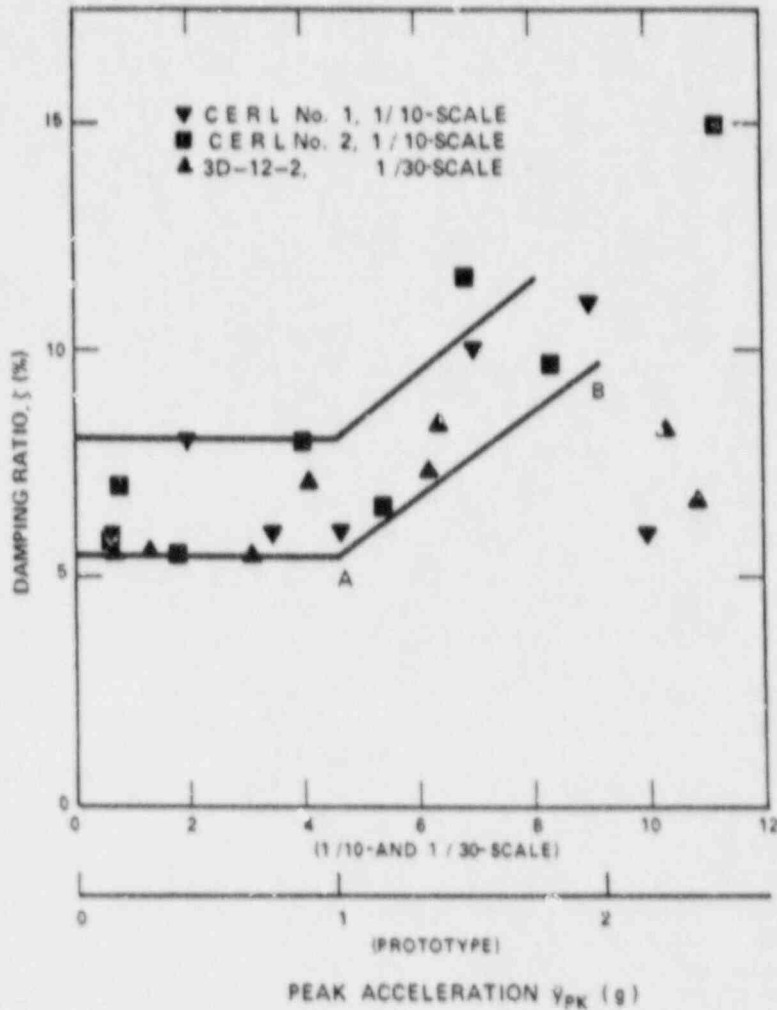
Fig. 15. Measured damping ratios determined from real part of the frequency response function for diesel generator building models.

Damping ratios shown in Fig. 15 represent the modal damping value associated with the fundamental frequency of the structure. Although these damping ratios should be used with the complex eigenvalue methods of solution for the modal response, they should also be applicable to the modal damping ratios associated with proportional damping in an equivalent energy-loss sense.

All the frequency response functions were calculated from simulated seismic base excitations in the horizontal direction and from the associated floor responses in the same direction. Similar analysis of the frequency response functions measured on the 1/42-scale auxiliary building model showed modal

damping values of 2-5% for the first mode. The damping values measured on
TRG-1 and TRG-3 that were identified from the frequency response function
plots and that were associated with the first mode are summarized in Tables X
and XI.

TABLE X

TRG-1 1ST MODE DAMPING RATIOS IDENTIFIED FROM REAL PART OF THE FREQUENCY RESPONSE FUNCTION

Excitation Level[*] (g's)	Modal Damping Ratio (% of Critical)
0.50	3.3
0.80	3.3
0.96	3.4
4.16	6.0
4.84	7.6
8.88	8.8

[*] Peak acceleration base input from a time-scaled
version of the 1940 El Centro earthquake.

TABLE XI

TRG-3 1ST MODE DAMPING RATIOS IDENTIFIED FROM REAL PART OF THE FREQUENCY RESPONSE FUNCTION

Excitation Level[*] (g's)	Modal Damping Ratio (% of Critical)
0.12	7.0
0.87	6.0
0.99	11.0
1.47	6.0
1.65	7.0
2.46	7.0
2.59	8.0
4.48	8.0

[*] Peak acceleration base input from a time-scaled
version of the 1940 El Centro earthquake.

V. OTHER INVESTIGATOR RECOMMENDATIONS AND DESIGN STANDARD RECOMMENDATIONS FOR DAMPING IN REINFORCED CONCRETE STRUCTURES

Currently, NRC Regulatory Guide 1.61[16] specifies an equivalent viscous damping ratio of 4% of critical for operating basis earthquakes or half-safe shutdown earthquakes and a damping ratio of 7% of critical for safe shutdown earthquakes. Housner[17] suggested that a damping ratio of 5% of critical be used for reinforced concrete. This value was independent of the stress levels in the structure or of the intensity of the earthquake. Newmark[18] suggested damping values for reinforced concrete that are a function of the stress level. These values range from 0.5 - 1.0% of critical at stress levels less than 25% of yield to 10-15% of critical when stress levels are such that permanent deformations are produced. Stevenson[19] provides a summary of the damping values used by the nuclear industry for both mechanical and structural components. For reinforced concrete shear wall structures that were tested at stress levels less than 25% of yield, damping ratios ranged from 1.5% to 12.5% of critical, with an average value of 5.2%. This reference also quantifies the change in the damping of reinforced concrete shear walls with strain in the reinforcement and suggests a method for calculating damping values as a function of deformation, stress, or strain level. Free vibration tests on shear walls that were performed by the Portland Cement Association are summarized in Ref. (20). Initially, the displacements used in the pluck tests before any static load cycling were less than 36% of the displacements required to yield the structure. Damping during these free vibration tests ranged from 2.0 - 3.6% of critical. The free vibration tests were repeated after damage had been introduced into the walls by static, cyclic testing. A similar initial displacement was used for the tests, and damping was shown to increase with the amount of damage in the walls. Damping measured in the damaged walls was as high as 14.5% of critical. Free vibration tests were also performed by Shiga, et al.,[21] on low aspect ratio shear walls enclosed by a reinforced concrete frame. Damping values of 3% of critical were measured.

The standard of The American Society of Civil Engineer's for Seismic Analysis Related Nuclear Structures[22] recommends the same damping values as NRC Regulatory Guide 1.61. This standard will allow increased damping values, if they can be properly justified.

VI. CONCLUSIONS

The damping values measured in this program for reinforced concrete show reasonably consistent trends. Before first cracking of the structures (i.e., "yield"), equivalent viscous damping as a percentage of critical damping is generally between 3% and 8% and is higher for higher stress levels. It is also evident that the hysteretic values are generally lower than those values found by the other methods at the higher stress levels when expressed as equivalent viscous damping. This fact probably reflects that damping measured in this manner neglects other energy losses that are velocity dependent in the non-linear region. It is likely that, if all known data are plotted as a function of nominal stress level, a clear trend will be exhibited (although this method should not be used to develop a stress-dependent expression because of the stress variation throughout all known tests). This trend would indicate that a stress-dependent expression can be developed, if experiments are carried out under uniform stress conditions.

It is noted that consistent values were obtained, even though a remarkably different set of methods were used to evaluate the energy losses. In this regard, the response spectra matching method used here is the first known application of this technique for quantifying damping from experimental data. Clearly, this method is very general and powerful in that all damping mechanisms are included in the final evaluation. We believe this method has considerable merit.

VII. REFERENCES

1. E. G. Endebrock, R. C. Dove, and W. E. Dunwoody, "Analysis and Tests on Small-Scale Shear Walls, FY-82 Final Report," Los Alamos National Laboratory report, NUREG/CR-4274, September 1985.

2. R. C. Dove, J. G. Bennett, C. R. Farrar, and C. A. Anderson, "Seismic Category I Structures Program: Results for Fiscal Years 1983-84, FY 83-84 Report," Los Alamos National Laboratory report, NUREG/CR-4924, September 1987.

3. J. G. Bennett, et al., "Simulated Seismic Tests on 1/42- and 1/14-Scale Category I Auxiliary Building," Los Alamos National Laboratory report, NUREG/CR-4987, October 1987.

4. J. G. Bennett, et al., "Seismic Category I Structures Program: Results for FY 85," Los Alamos National Laboratory report, NUREG/CR-4998, December 1987.

5. J. G. Bennett, et al., "Seismic Category I Structures Program: Results for FY 86," Los Alamos National Laboratory report, in preparation.

6. J. G. Bennett, et al., "Seismic Category I Structures Program: Results for FY 87," Los Alamos National Laboratory report, in preparation.

7. W. C. Hurty and M. F. Rubinstein, Dynamics of Structures, (Prentice-Hall, Inc., Englewood Cliffs, New Jersey, 1964).

8. J. E. Ruzicka and T. F. Derby, Influence of Damping In Vibration Isolation, (The Shock and Vibration Information Center, Washington, D.C., 1971).

9. S. Timoshenko, D. Young, and W. Weaver, Jr., Vibration Problems in Engineering, (John Wiley & Sons, New York, 1974).

10. W. Thomson, Theory of Vibrations With Applications, (Prentice-Hall, Inc., Englewood Cliffs, New Jersey, 1981).

11. R. Clough and J. Penzien, Dynamics of Structures, (McGraw-Hall, Inc., New York, 1975).

12. Committee on Nuclear Structures and Materials, Structural Analysis and Design of Nuclear Power Plant Facilities, (American Society of Civil Engineers, New York, 1980).

13. L. Meirovitch, Computational Methods in Structural Dynamics, (SIJTHOFF & NOORDHOFF), Rockville, MD, 1980.

14. R. Dove and J. G. Bennett, "Scale Modeling of Reinforced Concrete Category I Structures Subjected to Seismic Loading," Los Alamos National Laboratory Report NUREG/CR-4474.

15. D. Ewins, Modal Testing: Theory and Practice, (John Wiley & Sons, Inc., New York, 1984).

16. Division of Nuclear Regulatory Standards, "Damping Values for Seismic Design of Nuclear Power Plants, Reg. Guide 1.61," (United States Nuclear Regulatory Commission, Washington, D.C., 1973).

17. G. W. Housner, R. R. Martel and J. L. Alford, "Spectrum Analysis of Strong-Motion Earthquakes," Bull. Seismo. Soc. Am., 43, pp. 97-119. (1953).

18. H. Newmark and W. Hall, "Seismic Design Criteria for Nuclear Reactor Facilities," in Proc. 4th World Conference on Earthquake Engineering, B4, pp. 37-50. (Santiago, Chile, 1969).

19. J. D. Stevenson, "Structural Damping Values as A Function of Dynamic Response Stress and Deformation Levels," Nuclear Eng. and Design, 60, pp. 211-238, (1980).

20. J. Aristizabal-Ocloa, "Cracking and Shear Effects on Structural Walls," J. of Structural Div., ASCE, 109, No. 5, pp. 1267-1277, (May, 1985).

21. T. Shiga, A. Shibata, and J. Takahashi, "Experimental Study On Dynamic Properties of Reinforced Concrete Shear Walls," Proc. World Conf. on Earthquake Engineering, 5th, Rome, 1973, 1, pp 1152-1166.

22. Committee on Nuclear Standards, Seismic Analysis of Safety-Related Nuclear Structures, (ASCE, New York, 1987).

2. TITLE AND SUBTITLE	3. LEAVE BLANK
Experimental Assessment of Damping in Low Aspect Ratio, Reinforced Concrete Shear Wall Structures	

5. AUTHOR(S)

Charles R. Farrar
Joel G. Bennett

4. DATE REPORT COMPLETED	
MONTH	YEAR
April	1988

6. DATE REPORT ISSUED	
MONTH	YEAR
August	1988

7. PERFORMING ORGANIZATION NAME AND MAILING ADDRESS (Include Zip Code)

Los Alamos National Laboratory
Box 1663
Los Alamos, NM 87545

8. PROJECT/TASK/WORK UNIT NUMBER

9. FIN OR GRANT NUMBER

A7221

10. SPONSORING ORGANIZATION NAME AND MAILING ADDRESS (Include Zip Code)

Division of Engineering
Office of Nuclear Regulatory Research
U.S. Nuclear Regulatory Commission
Washington, DC 20555

11a. TYPE OF REPORT

Technical

b. PERIOD COVERED (Inclusive dates)

12. SUPPLEMENTARY NOTES

13. ABSTRACT (200 words or less)

This report summarizes the experimental data obtained from the Seismic Category I Structures Program concerning damping in low aspect ratio, reinforced concrete shear wall structures. This program, that is sponsored by the United States Nuclear Regulatory Commission, has tested 37 shear wall structures and structures and structural elements both statically (monotonic and cyclic) and dynamically (sine sweep, random, simulated seismic, and impulse). Data from these tests have been analyzed by four different methods to determine equivalent viscous damping ratios that can be used in the analysis of shear wall structures. These methods are: (1) Frequency response function analysis, (2) The log decrement method, (3) The hysteretic energy loss method, and (4) The flow response spectra matching method. The flow response matching method is, to the author's knowledge, new and provides the most general method for assessing a variety of damping mechanisms. Results from the various methods were generally consistent and the damping values were found to be in the range specified by current regulatory guides. A discussion of the various damping mechanisms, how damping mechanisms affect the equations of motion, the effects of the type of loading on the various methods used to determine the damping, and other investigators' results are also presented.

14. DOCUMENT ANALYSIS - a. KEYWORDS/DESCRIPTORS

damping
shear wall structure
low aspect ratio

b. IDENTIFIERS/OPEN-ENDED TERMS

15. AVAILABILITY STATEMENT

Unlimited

16. SECURITY CLASSIFICATION

(This page)
Unclassified

(This report)
Unclassified

17. NUMBER OF PAGES

18. PRICE

UNITED STATES
NUCLEAR REGULATORY COMMISSION
WASHINGTON, D.C. 20555

———

OFFICIAL BUSINESS
PENALTY FOR PRIVATE USE, $300

EXPERIMENTAL ASSESSMENT OF DAMPING IN LOW ASPECT RATIO, REINFORCED CONCRETE SHEAR WALL STRUCTURE

AUGUST 1988